ChemComm

COMMUNICATION

View Article Online
View Journal | View Issue

Cite this: *Chem. Commun.*, 2014, 50, 1719

Received 22nd November 2013,
Accepted 6th December 2013

DOI: 10.1039/c3cc48919a

www.rsc.org/chemcomm

Metal tips on pyramid-shaped PbSe/CdSe/CdS heterostructure nanocrystal photocatalysts: study of Ostwald ripening and core/shell formation†

Whi Dong Kim,[a] Sooho Lee,[a] Chaewon Pak,[a] Ju Young Woo,[a] Kangha Lee,[a] Fábio Baum,[a] Jonghan Won[b] and Doh C. Lee*[a]

We report ripening of metal particles anchored on pyramid-shaped heterostructure nanocrystals. The 'intra-particle' ripening results in a large metal tip at one corner with the other three tips vanishing. Investigation reveals that the ripening and core/shell formation affects photocatalytic activities *via* the Fermi level change.

Metal nanoparticles deposited on the surface of semiconductor photocatalysts enhance their photocatalytic activity. With their surface partially coated with small metal particles, semiconductor colloids show enhanced photocatalytic performance in various reactions, such as water splitting,[1,2] reduction of carbon dioxide,[3] and degradation of phenol.[4] The metal cocatalysts serve as both electron sinks and catalytic reaction sites, in which the metal/semiconductor interfaces facilitate the separation of the photogenerated electron and hole.[5] Recently, a growing demand for the development of photocatalysts for energy applications has fueled the search for optimal metal–semiconductor combinations.[6–8]

Colloidal lead selenide (PbSe) nanocrystal quantum dots have been used for photocatalysis under infrared irradiation.[9] The growth of cadmium chalcogenide shell layers on a PbSe quantum dot provides electronic energy levels in the staggered offset (type II) configuration, which could offer a platform for efficient charge separation.[10] In addition, the synthesis of "open"-structure heterostructure nanocrystals (HNCs), such as nanopyramids or nanotetrapods, is possible because of the anisotropy of the wurtzite CdS crystals. The very anisotropy helps the HNCs anchor metal particles at the tips. For example, Au nanoparticles could grow selectively at tips of anisotropic CdS nanocrystals.[11,12] The junction between semiconductor nanocrystals and metal tips remains relatively tenacious, until the metal nanoparticles undergo ripening.

Here, we investigate the photocatalytic activity of pyramid-shaped PbSe/CdSe/CdS HNCs with varying geometries and compositions of metal cocatalysts deposited on their surface. In an attempt to address the question, "How does the work function of a metal cocatalyst affect photocatalytic pathways in metal-tipped PbSe/CdSe/CdS pyramid HNCs?", we have introduced the ripening of metal tips on pyramid-shaped PbSe/CdSe/CdS core/shell/shell HNCs, and its effect on photocatalytic reactions. We also report the Au/Ag core/shell metal tips, whose work functions can also be controlled with their geometric configuration.

Our initiative started with changing the size of Au tips grown on the HNCs. One obvious approach to growing larger metal nanoparticles in a colloidal reaction is to increase the concentration of the metal precursor in the solution: the higher the concentration, the larger the tips. Fig. 1 shows transmission electron microscopy (TEM) images of Au-tipped PbSe/CdSe/CdS pyramid HNCs with varying $HAuCl_4$ concentrations. At a low Au concentration (Au : HNC = 1200 : 1),[13] four Au tips grow at the corners of pyramid HNCs (Fig. 1b). The selective growth at the corners is a consequence of the high reactivity of (111) planes of zinc blende CdS at pyramid tips (see Fig. S1, ESI†), which are atomically identical to the (001) planes of wurtzite CdS.[14,15] Interestingly, when Au concentration increases (Au : HNC = 2300 : 1), one Au tip grows at the expense of the three other particles on each HNC (Fig. 1c and d). In the discussions that follow, we denote the ripened Au-tip HNCs as rAu–HNCs. The ripening appears to take place in an "intra-particle" fashion; namely, the Au atoms travel only within their host HNC, so each HNC ends up with one larger Au tip. This *winner-take-all* motif of Au tip ripening was previously observed in Au–CdSe nano-dumbbells, where asymmetric Au growth occurs at higher Au concentration.[16,17] The Au tips undergo ripening in an "intra-particle" fashion because the host CdSe nanorods are considered to serve as electron conduction channels. Menagen *et al.* later supported the idea by providing indirect evidence of the electron transfer through CdSe/CdS core/shell nanorods in the process of Au ripening.[12]

The electron conduction model appears to explain the intra-particle ripening of Au in our system, shown in TEM images of Fig. 1. In an effort to eliminate ambiguity, we devised a simple

[a] *Department of Chemical and Biomolecular Engineering, KAIST Institute for the Nanocentury, Korea Advanced Institute of Science and Technology (KAIST), Daejeon 305-701, Korea. E-mail: dclee@kaist.edu*
[b] *Division of Electron Microscopic Research, Korea Basic Science Institute, Daejeon 305-333, Korea*

† Electronic supplementary information (ESI) available: Detailed description of experimental procedures, TEM image of the photoreduction process in the dark. Elemental analysis of Ag–Au–HNCs. See DOI: 10.1039/c3cc48919a

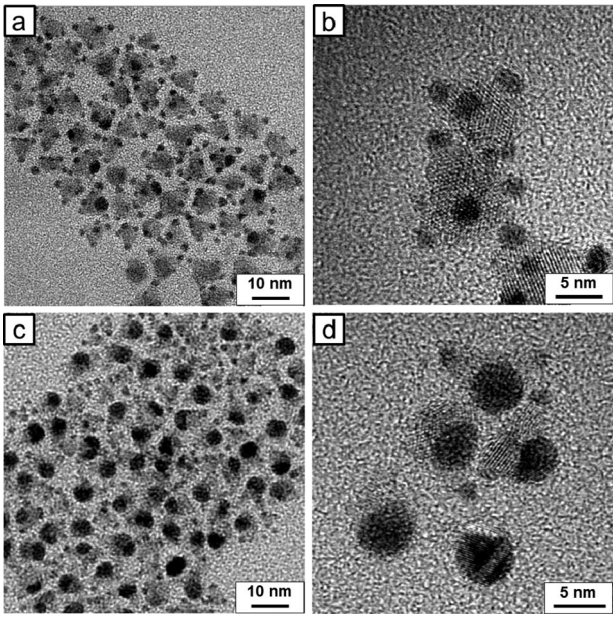

Fig. 1 TEM images of Au-tipped PbSe/CdSe/CdS HNCs. (a, b) Au–HNCs after adding low concentration of gold precursors to the HNCs (Au : HNC = 1200 : 1) and (c, d) rAu–HNCs after adding a relatively high concentration of $HAuCl_4$ (Au : HNC = 2300 : 1).

experiment, in which a Cu wire coated with Au-tipped HNCs was immersed in the Au precursor solution and the Au reduction proceeded (Fig. 2a). Now, the electron would be able to travel "between" pyramid HNCs as the Cu wire serves as a charge carrier conduction channel. Fig. 2b and c shows TEM images of the product collected from the Cu wire before and after the ripening process. 2 nm of gold nanoparticles are evenly deposited on each pyramid HNC before the ripening process (Fig. 2b), while Au tips appear to undergo ripening (Fig. 2c). Note that some of the HNCs turned tip-free, while some HNCs have larger Au tips (some with 3 tips). Now, the conductive channel between HNCs enables the "cross-particle" ripening, in which a larger Au tip on a HNC can grow at the expense of a smaller tip on another HNC. Fig. 3 illustrates the contrast between the Ostwald ripening processes with and without the Cu conductive substrate in our system. The impetus for the Ostwald ripening on conducting substrates derives from the difference in work function between the Au particles of different sizes.[18]

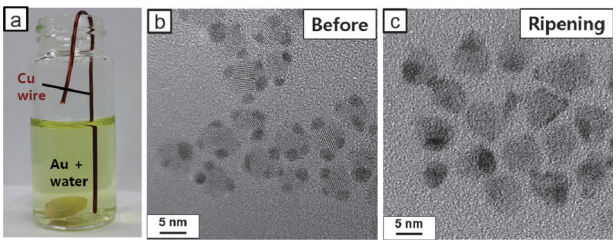

Fig. 2 (a) Photograph of experimental setup for Au growth on HNCs with Cu wire immersed in the solution. (b, c) TEM images of HNCs before and after Au-tip growth: (b) before adding $HAuCl_4$; (b) Au-tipped HNCs; and (c) Au–HNCs after 30 min of growth. Inter-particle ripening takes place as the Cu wire, a conductive substrate, helps electrons to travel between HNCs. As a result, some HNCs have no Au tips while other HNCs have multiple large Au tips.

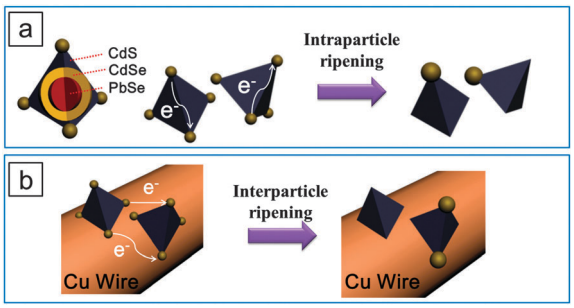

Fig. 3 Illustration of the Ostwald ripening of gold nanoparticles on (a) free-standing pyramid-shaped HNCs and (b) the Au–HNCs anchored on a conductive substrate, *e.g.*, a Cu wire.

When no conductive substrate was introduced, two primary changes in the Au tips occur as a result of the Ostwald ripening: (i) the number of Au tips attached on each HNC decreases (*i.e.*, four to one), and (ii) the size of the remaining Au tip increases. Both of the changes could play a role in altering the photocatalytic activity. To elucidate the effects, we prepared several types of Au–HNC hybrid photocatalysts and tested their photocatalytic activity in the reduction of methylene blue (MB) under 785 nm light irradiation: pyramid-shaped PbSe/CdSe/CdS HNCs with no Au tips (denoted as HNCs), HNCs with 1.7 nm Au tips (Au–HNCs), and HNCs with ripened Au at one corner (rAu–HNCs). The concentration of MB in the MB–photocatalyst mixture was estimated from the absorption spectra: the optical density (OD) at 650 nm subtracted from the OD contributed by the photocatalysts. Typically, the absorption spectra of MB–photocatalyst samples show a peak at ~650 nm characteristic of MB, and the peak diminishes as a consequence of the photocatalytic reduction of MB (Fig. S2, ESI†). For example, in the case of Au–HNCs, 4 h of irradiation at 785 nm resulted in the reduction of 57% of MB *versus* 19% in the case of HNCs (Fig. 4a). Au tips serve as an electron sink and consequently facilitate charge separation at the semiconductor–metal interfaces.[9]

In addition to the photocatalytic reduction of MB, we used our HNC-based hybrid materials for the photoreduction of metal salts to metal particles. First, we attempted photocatalytic reduction of $AgNO_3$ using the PbSe/CdSe/CdS HNCs. As shown in Fig. 5a, ~3 nm

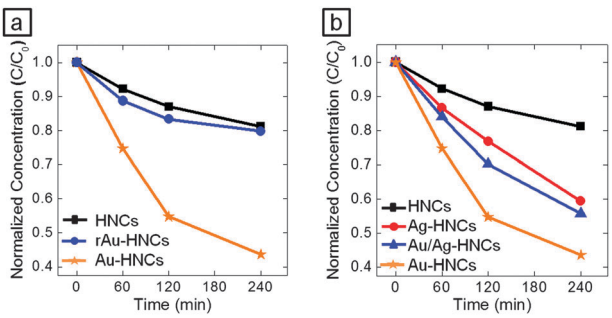

Fig. 4 (a) Normalized concentration of MB after exposure to 785 nm light with Au-tipped pyramidal PbSe/CdSe/CdS HNCs as a function of reaction time. rAu–HNCs show lower photocatalytic activity than Au–HNCs and even HNCs. (b) Photocatalytic conversion with Au–HNCs (orange, star), Ag–HNCs (red, circle), rAu–HNCs (black, square), and Au–Ag core–shell HNCs (blue, triangle). A 785 nm laser was used as the irradiation source in the photocatalysis.

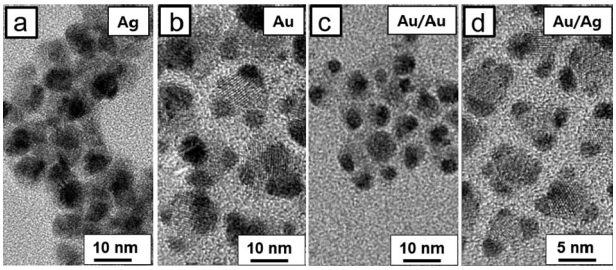

Fig. 5 TEM images of HNCs with (a) $AgNO_3$ and (b) $HAuCl_4$ reduced under irradiation at 530 nm for 30 min. Photocatalytic reduction results in the growth of large Ag and Au particles, respectively. TEM images in (c) and (d) show Au–HNCs that undergo further growth with $HAuCl_4$ and $AgNO_3$, respectively, under irradiation at 530 nm.

sized Ag tips grew at the corners of the HNCs even when no reducing agent was used, after the HNCs and $AgNO_3$ mixture solution was placed under irradiation at 530 nm for 30 min. On the other hand, almost no Ag particles were reduced in the dark (Fig. S3a, ESI†). Under room light, 1–2 nm sized Ag tips were grown on the pyramid-shaped HNCs (Fig. S3c, ESI†). This indicates that Ag tip growth occurs more rapidly through photoreduction than Ag cation exchange.[19,20] Interestingly, other reports claim that cation exchange from Cd^{2+} to Ag^{+} is relatively fast.[21] The sharp contrast likely results from the activated photoreduction under our experimental conditions due to the presence of hole scavengers. When $HAuCl_4$ is used, large Au nanoparticles are formed after 30 min of irradiation under 530 nm, similar to the case of the Ag growth (Fig. 5b). Notably, small Au tips on HNCs do not disappear while the ripening appears to have occurred, unlike the ripening that occurred under room light (see Fig. 1c and d). The average volume of Au per HNC obviously increased (12 nm^3 *vs.* 62 nm^3), which is attributed to the facilitated growth of the Au tips *via* photocatalyzed reduction of $HAuCl_4$. $HAuCl_4$ could also be reduced by oleylamine, which is a mild reducing agent, present on or near the surface of HNCs, as hinted from a control experiment in which HNCs were mixed with $HAuCl_4$ in the dark and small Au tips grew (Fig. S3b, ESI†).[22,23]

Fig. 5c and d show TEM images of hybrid nanoparticles after further growth of Au and Ag on Au–HNCs, respectively. After 5 min of irradiation, $HAuCl_4$ was reduced on the Au tips, as evidenced from the increased size of Au tips. When $AgNO_3$ was used, Ag shells grew on the Au tips. This core/shell formation was confirmed by elemental analysis with increase in the average volume of metal tips per HNC (Fig. S4, ESI†). Then, we monitored the photocatalytic reduction of MB with the prepared metal–HNC hybrid particles under 785 nm light irradiation (Fig. 4b). Au–HNCs show higher photocatalytic activity than Ag–HNCs (HNCs with Ag tips). We attribute this difference to the difference of work function and surface reactivity of the two metals: *i.e.*, Au and Ag ($\Phi_{Au} = -5.1$ eV, $\Phi_{Ag} = -4.5$ eV). In the case of the Au/Ag core/shell structure, the activity level for the photocatalytic reaction seems to be positioned in between the cases of Au and Ag. The photocatalytic efficiency of Ag–Au–HNCs would thus fall in between the cases of Au–HNCs and Ag–HNCs. The Au/Ag–HNCs show saturation in terms of photocatalysis at around 90 min, which is a ramification of poor colloidal stability after multi-Ag shell growth steps.

In conclusion, we have demonstrated that varying geometries of Au and Ag tips on the pyramid-shaped PbSe/CdSe/CdS HNCs influence the photocatalytic activity of the hybrid composites. The Ostwald ripening and subsequent photoreduction of metal salts in the presence of free-floating HNCs enable the versatile control of metal tips with geometric configurations ranging from ripened single metal tip to core/shell metal nanoparticles. rAu–HNCs have larger single Au tips per HNC, as opposed to four smaller tips in the case of Au–HNCs. The ripening of the metal tips on pyramid-shaped HNCs reduced the photocatalytic activity of HNCs. The work function could be controlled through the core/shell metal tip growth *via* alternating photoreduction. The control of the Fermi level of metal tips would enable the improved photocatalytic conversion particularly when the reaction steps involved multiple intermediates (*e.g.*, CO_2 conversion).

The authors acknowledge the National Research Foundation (NRF) grant (No. 2013-026083 and 2012-0009650) and by the New & Renewable Energy of the Korea Institute of Energy Technology Evaluation and Planning (KETEP) grant funded by the Korea Ministry of Trade, Industry and Energy (No. 20133010011750) (Dongjin Semichem Co., LTD.).

Notes and references

1 H. Park, W. Choi and M. R. Hoffmann, *J. Mater. Chem.*, 2008, **18**, 2379.
2 T. A. Kandiel, A. A. Ismail and D. W. Bahnemann, *Phys. Chem. Chem. Phys.*, 2011, **13**, 20155.
3 X. J. Feng, J. D. Sloppy, T. J. LaTemp, M. Paulose, S. Komarneni, N. Z. Bao and C. A. Grimes, *J. Mater. Chem.*, 2011, **21**, 13429.
4 R. Su, R. Tiruvalam, Q. He, N. Dimitratos, L. Kesavan, C. Hammond, J. A. Lopez-Sanchez, R. Bechstein, C. J. Kiely, G. J. Hutchings and F. Besenbacher, *ACS Nano*, 2012, **6**, 6284.
5 M. R. Hoffmann, S. T. Martin, W. Y. Choi and D. W. Bahnemann, *Chem. Rev.*, 1995, **95**, 69.
6 L. Amirav and A. P. Alivisatos, *J. Phys. Chem. Lett.*, 2010, **1**, 1051.
7 A. Wood, M. Giersig and P. Mulvaney, *J. Phys. Chem. B*, 2001, **105**, 8810.
8 V. Subramanian, E. Wolf and P. V. Kamat, *J. Phys. Chem. B*, 2001, **105**, 11439.
9 C. Pak, J. Y. Woo, K. Lee, W. D. Kim, Y. Yoo and D. C. Lee, *J. Phys. Chem. C*, 2012, **116**, 25407.
10 D. C. Lee, I. Robel, J. M. Pietryga and V. I. Klimov, *J. Am. Chem. Soc.*, 2010, **132**, 9960.
11 A. E. Saunders, I. Popov and U. Banin, *J. Phys. Chem. B*, 2006, **110**, 25421.
12 G. Menagen, D. Mocatta, A. Salant, I. Popov, D. Dorfs and U. Banin, *Chem. Mater.*, 2008, **20**, 6900.
13 Au : HNC denotes the ratio of the number of Au atoms to that of HNCs. See ESI† for the description of the estimate detailed.
14 L. Manna, D. J. Milliron, A. Meisel, E. C. Scher and A. P. Alivisatos, *Nat. Mater.*, 2003, **2**, 382–385.
15 S. E. Habas, P. D. Yang and T. Mokari, *J. Am. Chem. Soc.*, 2008, **130**, 3294.
16 T. Mokari, C. G. Sztrum, A. Salant, E. Rabani and U. Banin, *Nat. Mater.*, 2005, **4**, 855.
17 N. Mishra, J. Lian, S. Chakrabortty, M. Lin and Y. Chan, *Chem. Mater.*, 2012, **24**, 2040.
18 P. L. Redmond, A. J. Hallock and L. E. Brus, *Nano Lett.*, 2005, **5**, 131.
19 S. Chakrabortty, J. A. Yang, Y. M. Tan, N. Mishra and Y. Chan, *Angew. Chem., Int. Ed.*, 2010, **49**, 2888.
20 P. Rukenstein, I. J.-L. Plante, M. Diab, E. Chockler, K. Flomin, B. Moshofsky and T. Mokari, *CrystEngComm*, 2012, **14**, 7590.
21 D. H. Son, S. M. Hughes, Y. Yin and A. P. Alivisatos, *Science*, 2004, **306**, 1009.
22 Y. Yang, Y. Yan, W. Wang and J. R. Li, *Nanotechnology*, 2008, **19**, 1.
23 H. Tada, A. Takao, T. Akita and K. Tanaka, *ChemPhysChem*, 2006, **7**, 1687.